Environmental Science
Processes & Impacts

Effects of carbonate on the ferrihydrite transformation in alkaline media

Journal:	*Environmental Science: Processes & Impacts*
Manuscript ID	EM-ART-10-2023-000469.R2
Article Type:	Paper

Environmental Significance

Alkaline media widely exist in natural and engineered systems, where carbonate content is increasing due to the substantial increased atmospheric carbon dioxide concentration. In the meantime, ferrihydrite commonly occurs and profoundly influences the fate of nutrients and contaminants, but easily transform into more crystalline minerals. Compared with the strong inhibitory effect on the ferrihydrite transformation induced by other oxyanions (e.g., phosphate, silicate, and arsenic), this study clearly demonstrates the different behavior of carbonate. Although carbonate slowed down the ferrihydrite transformation slightly and suppressed the goethite formation, it promoted the hematite formation regardless of its concentration, which may potentially provide a pathway for hazardous elements retention. These results highlight the importance of carbonate controlling the transformation and occurrence of iron (oxyhydr)oxides. This study improves the understanding of the complex iron and carbon cycles under the scenario of climate change.

Effects of carbonate on the ferrihydrite transformation in alkaline media

Ying Li,*[ab] Chaoqun Zhang,[c] Meijun Yang,[c] Jing Liu,[d] Hongping He,[c] Yibing Ma[a] and Yuji Arai[b]

[a] *National Observation and Research Station of Coastal Ecological Environments in Macao; Macao Environmental Research Institute, Faculty of Innovation Engineering, Macau University of Science and Technology, Macao SAR 999078, China*

[b] *Department of Natural Resources and Environmental Sciences, University of Illinois at Urbana-Champaign, Urbana, IL 61801, USA*

[c] *CAS Key Laboratory of Mineralogy and Metallogeny/Guangdong Provincial Key Laboratory of Mineral Physics and Materials, Guangzhou Institute of Geochemistry, Chinese Academy of Sciences, Guangzhou 510640, China*

[d] *State Key Laboratory of Lunar and Planetary Sciences, Macau University of Science and Technology, Taipa 999078, Macau*

* *Corresponding author*

Email address: liying@must.edu.mo

† Electronic supplementary information (ESI) available. See DOI: XXX.

Abstract

Alkaline media widely exist in natural and engineered systems such as semiarid/arid areas, radioactive waste sites, and mine tailings. At these settings, the commonly occurred iron

(oxyhydr)oxides differed in their ability to influence the fate of nutrients and contaminants. Due to the substantial increased atmospheric carbon dioxide (CO_2) concentration, carbonate stands to increase in these media. However, how increasing carbonate affects the transformation of poorly crystalline iron (oxyhydr)oxides (e.g., two-line ferrihydrite) under alkaline condition still remains unclear. Here, kinetics of ferrihydrite transformation were evaluated at pH ~10 as a function of [carbonate] = 0-286 mM using synchrotron-based X-ray and vibrational spectroscopic techniques. Results showed that carbonate slowed down the ferrihydrite transformation slightly and suppressed the goethite formation, but promoted the hematite formation regardless of its concentration. At low carbonate addition (11.42 mM), the effect of carbonate on the product formation was obvious due to the weak inner-sphere complex, however, at high carbonate concentration (80-286 mM), the effect was retarded because of the adsorption equilibrium of carbonate as well as the initial carbonate adsorption followed by desorption. Moreover, carbonate modified the morphology of hematite from rhombic to ellipsoidal to honeycomb and goethite from rod-like to needle-like to rugby-like due to the inner-sphere adsorption-desorption of carbonate and adsorption of hydroxyl ions on reactive sites of iron (oxyhydr)oxides in alkaline media. Results suggest that the concurrent increasing carbonate with enhanced atmospheric CO_2 could control the transformation and occurrence of iron (oxyhydr)oxides in natural and engineered environments and have important implications for the biogeochemical cycles of iron and carbon.

Keywords: Carbonate, Ferrihydrite, Transformation, Alkaline media, Hematite, Goethite

1. Introduction

Alkaline media are important environmental matrices in natural and engineered systems. For example, alkaline soils are common in semiarid and arid areas, covering more than 25 % of the Earth's surface.[1] Alkaline environments exist in high-level radioactive/nuclear waste disposal sites, mine tailings, and metallurgical operations.[2, 3] Besides, acid mining raffinate was always treated via neutralization by adding slaked lime to increase the pH to alkaline and induce mineral precipitation.[4, 5] At these settings, iron (oxyhydr)oxides commonly occur and profoundly influence the fate, bioavailability, and toxicity of environmental contaminants.[6, 7] However, different iron (oxyhydr)oxides differed in their ability to affect contaminants and nutrients. For example, two-line ferrihydrite (hereafter called ferrihydrite) is the initial iron oxyhydroxide precipitate by the rapid hydrolysis of Fe(III) and exhibits superior sorption properties for several hazardous elements (e.g., As, Cr, Pb, and Cd) due to its extremely high surface area and reactivity.[8-12] However, it is an unstable solid, and at alkaline pH 10-13, it rapidly transforms to goethite with minor hematite via dissolution and recrystallization.[13-15] The generated goethite and hematite show lower adsorption capacity towards environmental substances.[16, 17] And with ferrihydrite transformation, hazardous elements (e.g., U, As, and Pb) could be incorporated into the structure of hematite.[3, 4, 18]

As one of the most important greenhouse gases, concentration of carbon dioxide (CO_2) in the atmosphere is increasing rapidly at the rate of 2.0 ± 0.1 ppmv/year due to the human activities.[19] The increasing atmospheric CO_2 entails increased carbonate in alkaline soils, where can store a large amount of carbonate anions and carbon because alkaline pH favors the

dissolution of CO_2 and precipitation of carbonate.[20-22] This is regarded as a promising carbon removal strategy. In engineered systems, when pH of geochemical environments is artificially adjusted during remediation, the concentration of carbonate gradually increases to ~180 mM at pH 10 under air-equilibrated system (pCO_2 = 408 ppmv).[23] The increasing carbonate concentration/activity exhibits significant impacts on elemental dynamics and further influence environmental geochemical cycles. For example, carbonate can enhance or suppress the adsorption and/or incorporation of common cations (e.g., Pb(II), Mn(II), and U(VI)) and anions (e.g., arsenic, chromate, and selenate) on minerals via competing for the reactive sites on mineral surfaces, forming carbonate complexes and/or precipitates.[24-27] However, the effects of carbonate on the transformation of poorly crystalline minerals (e.g., ferrihydrite) under alkaline conditions remains poorly understood.

The objectives of this study were to investigate the impacts of carbonate on the ferrihydrite transformation in alkaline media and elucidate the involved mechanisms. Batch aqueous geochemical experiments were conducted in conjunction with advanced spectroscopic characterization including X-ray absorption spectroscopy (XAS), X-ray diffraction (XRD), transmission electron microscopy (TEM), and Fourier transform infrared spectroscopy (FTIR). The results contribute a new understanding of poorly crystalline mineral transformation interacting with carbonate in natural and pollution managed alkaline environments (e.g., semiarid/arid areas, radioactive waste sites, and mine tailings).

2. Materials and methods

2.1. Chemicals

All reagents in this study were of ACS-grade, and all solutions were prepared using boiled ultrapure water (18.2 MΩ cm) to exclude CO_2 gas.

2.2. Ferrihydrite transformation in the presence of carbonate under alkaline condition

The batch kinetics of ferrihydrite transformation as a function of carbonate concentration (0, 11.42, 80, 180, and 286 mM) were conducted at pH 10 under 40 °C using a completely mixed closed system. Boiled and degassed water was used as a control (0 mM carbonate). Carbonate concentration of 180 mM represented the current atmospheric pCO_2 (408 ppmv) at pH 10, which was calculated using Visual MINTEQ version 3.1.[23] Carbonate concentrations of 11.42 and 80 mM below 180 mM were selected considering the fact that atmospheric CO_2 gas would not dissolve completely and/or be partially sequestrated by Ca-bearing minerals under alkaline conditions,[22] while that of 286 mM above 180 mM predicted the elevated atmospheric pCO_2.[19] A pH value, 10, was chosen to simulate the alkaline media such as radioactive waste sites and in-situ tailings.[4, 28]

Ferrihydrite was prepared based on the methods used by Schwertmann et al.[29] Briefly, it was synthesized by the titration of a 0.2 M $Fe(NO_3)_3 \cdot 9H_2O$ solution (dissolving 20.2 g $Fe(NO_3)_3 \cdot 9H_2O$ to 250 mL boiled ultrapure water) to pH ~10 using a CO_2 free 1.0 M NaOH solution. Carbonate as sodium bicarbonate ($NaHCO_3$, 1.0 M in stock solution) was added with desired volume (0, 5.71, 40, 90, 143 mL) once ferrihydrite formed to achieve carbonate

concentration of 0, 11.42, 80, 180, and 286 mM, respectively. Fifty (50) mL of 300 mM 3-(cyclohexylamino)-2-hydroxy-1-propanesulfonic acid (CAPSO) was added to control pH at 10.[30, 31] The volume of the mineral suspension was monitored and calculated. Additional boiled ultrapure water was added to achieve the final volume of 500 mL. Afterward, 30-50 mL mineral suspension was quickly vacuum filtered, washed using ultrapure water, followed by the freeze-dried and labeled as sample at 0d. The remaining suspension was divided into 30 mL polypropylene bottles and sealed without any head space (i.e., closed system) to maintain respective carbonate concentration. To expedite the transformation process and avoid the enhanced effect of high temperature on the hematite formation, 40 ° C was selected to conduct the mineral transformation experiments. The bottles were sealed and stored in an oven at 40 °C for aging. To recover the transformation products, each bottle was sacrificed at sampling intervals (2d, 4d, 7d, 10d, 14d, and 21d). Mineral suspensions were quickly vacuum filtered and then washed twice using ultrapure water to remove entrained salts. The precipitates were immediately frozen, freeze-dried, and ground for solid characterization. The experiments of ferrihydrite transformation were conducted for 21d because almost 100% ferrihydrite was transformed into goethite and hematite at 10d and the trends of carbonate effects on the ferrihydrite transformation and product formation were clear within 21d. More details are discussed in Section 3.1.

To test whether the residual nitrate on the surface of freshly prepared ferrihydrite exhibits effects on the ferrihydrite transformation, transformation experiments in the presence of low and high nitrate concentration (i.e., 0.32 and 268 mM) were conducted at pH 10. Ferrihydrite

was synthesized using the same method described above, followed by the addition of $NaNO_3$ stock solution (5.0 M) to achieve the respective $NaNO_3$ concentration.

2.3. Relative proportions of iron (oxyhydr)oxides

To quantify iron phases of aged iron (oxyhydr)oxides, Fe K-edge extended X-ray absorption fine structure (EXAFS) spectra were performed at beamline 12-BM at Advanced Photon Source, Argonne, IL. Recovered kinetic samples were diluted with boron nitride at ~3-8% total Fe by wt%. The mixture was poured in a nylon washer and sealed with Kapton tape. All measurements were performed at room temperature in transmission mode. Data were collected up to approximately 13.78 $Å^{-1}$ in *k* space. Two to three scans of each sample or reference were collected to achieve decent spectra quality, and the spectra were processed using an ATHENA software package.[32] Parallel EXAFS scans were normalized, averaged, and converted to k^3-weighted EXAFS spectra. The relative contents of different iron (oxyhydr)oxides were calculated by the linear combination fitting (LCF) of k^3-weighted EXAFS spectra using spectra of references (i.e., ferrihydrite, goethite, and hematite, Fig. S1) at a *k*-range of 2-10 $Å^{-1}$. The *k* range of 2-10 $Å^{-1}$ was chosen due to two reasons. On one hand, some noisy signals inconsistently appeared at *k* range above 10 $Å^{-1}$ of different samples, which may affect normalization/data reduction. On the other hand, the *k* range of 2-10 $Å^{-1}$ was consistent with previous investigations conducted at near-neutral pH so that direct comparisons can be made with these two studies.[34, 39]

2.4. Characterization

The phases of fresh ferrihydrite (0d) and its transformation products (21d) were confirmed by powder X-ray diffraction (XRD). XRD patterns were acquired on a D8 advance diffractometer (Brucker, Billerica, MA, USA) with Cu Kα radiation (40 kV and 40 mA). All powder samples were scanned between 10 and 80° 2θ at a step of 2° 2θ min^{-1}.

The morphology of fresh (0d) and aged (21d) ferrihydrite was observed on a FEI Talos F200S field-emission transmission electron microscopy (TEM, FEI Co., USA) at an acceleration voltage of 200 kV. The phases of elected samples were further analyzed through selected area electron diffraction (SAED) and fast Fourier transform (FFT) from high-resolution lattice-fringe images. The sonicated mineral suspensions in ethanol were deposited on carbon-coated copper grids, which were placed in the vacuum chamber for analysis after ethanol evaporated completely.

The adsorbed carbonate on iron (oxyhydr)oxides was characterized by Fourier transform infrared (FTIR) spectroscopy recording on a Bruker VERTEX 70v instrument (Bruker, USA). Powder samples were mixed with KBr (approximately 1:100, w/w) and pressed into a pellet. One hundred twenty-eight scans in a range of 400-4000 cm^{-1} with a resolution of 4 cm^{-1} in transmission mode were collected for each sample. The data were analyzed with an OPUS software and OriginPro 2019.

3. Results and discussion

3.1. Ferrihydrite transformation in the presence of carbonate

3.1.1. XRD analysis

The XRD patterns of selected fresh (0d) and aged (21d) ferrihydrite in the presence of carbonate are shown in Fig. 1. Freshly prepared solids synthesized at 0d in control (0 mM) and high carbonate concentration (286 mM) showed two broad peaks at ca. 34° and 61°, confirming the formation of two-line ferrihydrite (Figs. 1a and 1b). Only the characteristic reflections of goethite were identified in the control system (in the absence of carbonate, Fig. 1c), revealing that alkaline condition favored the formation of goethite, which is consistent with the findings of Schwertmann et al.[13-15] In the presence of carbonate (11.42 to 286 mM), the diagnostic reflections of both hematite and goethite were observed (Figs. 1d-1g), revealing that ferrihydrite transformed to goethite and hematite with time. Interestingly, as carbonate concentration increased from 0 to 11.42 mM, the reflection intensity of goethite decreased markedly; whereas as carbonate concentration increased to 286 mM, the reflection intensity of goethite increased (Figs. 1c-1g). However, compared with goethite, the variation of the reflection intensity of hematite with carbonate concentration showed the opposite trend (Figs. 1c-1g). The XRD patterns revealed that carbonate changed the content of ferrihydrite transformation products (i.e., goethite and hematite) remarkably.

3.1.2. EXAFS and transformation kinetics analysis

Since XRD patterns are not sensitive to quantify amorphous phases such as ferrihydrite, the LCF analysis of Fe K-edge EXAFS spectra were conducted (Figs. S2-S6). The relative

contents of ferrihydrite, goethite, and hematite as a function of aging time under different carbonate concentration are listed in Table S1 and summarized in Fig. 2. In keeping with other literatures,[33, 34] ferrihydrite transformation in the presence of carbonate within 10d were well fitted by a pseudo first-order rate model (Eq. (1), Table S2), and the goethite and hematite formation within 10d were adequately described by the rearrangement of the same pseudo first-order rate model (Eq. (2), Table S2):

$$\mathrm{In}\left(\frac{C}{C_0}\right) = -k_{obs}t \quad (1)$$

$$\mathrm{In}\left(1-\frac{C}{C_0}\right) = -k_{obs}t \quad (2)$$

where k_{obs} is the reaction rate constant (d^{-1}), C_0 is the percent ferrihydrite before phase transformation (100%), and C is the relative amount of ferrihydrite remaining or product generating at aging time t (d). Fig. 3 shows the correlation between the k_{obs} (d^{-1}) value of ferrihydrite, goethite, and hematite versus carbonate concentration.

Two types of parameters were used to characterize the extent and speed of ferrihydrite transformation and product generation, respectively. Specifically, the former type, transformation efficiency of ferrihydrite and generation ratio of products, were obtained from the LCF of EXAFS spectra (Figs. S2-S6), and the latter type, transformation rate of ferrihydrite and generation rate of products, were calculated based on the pseudo first-order rate models (Eqs. (1) - (2)). Both the LCF of EXAFS spectra and kinetics analysis indicated that in alkaline media carbonate inhibited ferrihydrite transformation slightly because it inhibited goethite

formation but promoted hematite formation. At carbonate concentration beyond 11.42 mM, the inhibitory effect on goethite and enhancement effect on hematite were retarded. For example, the transformation efficiency (rate) of ferrihydrite decreased from 100% (0.259 d^{-1}) to 80% (0.130 d^{-1}) as carbonate concentration increased from 0 to 11.42 mM and fluctuated in the range of 79-86% (0.112-0.130 d^{-1}) as carbonate concentration increased to 286 mM (Figs. 2A and 3). For the goethite formation, the generation ratio (rate) decreased markedly from 90% (0.213 d^{-1}) to 21% (0.025 d^{-1}) and reached minimum at 11.42 mM of carbonate, and then increased to 52% (0.059 d^{-1}) at 286 mM of carbonate (Figs. 2B and 3). For the hematite formation, the highest generation ratio (rate) reached 59% (0.077 d^{-1}) at 11.42 mM of carbonate, and it decreased with decreasing or increasing carbonate concentration (Figs. 2C and 3).

3.1.3. TEM analysis

The SAED patterns confirmed the ferrihydrite formation at 0d and FFT patterns proved the hematite and goethite generation after 21d of transformation (insets in Figs. 4A, 4B, 4C, and 4G). Under control (0 mM) and high carbonate concentration (286 mM) at 0d, SAED patterns clearly displayed two bright rings with lattice spacings of 1.5 and 2.5 Å, which were assigned to the (115) and (110) reflection planes of two-line ferrihydrite, respectively (insets in Figs. 4A and 4B). For the aged ferrihydrite under 0 mM of carbonate, both hematite and goethite were detected. For instance, the fringe spacings of 2.53 and 1.48 Å corresponded to the *d*-value of (110) and (214) reflection planes of hematite at a zone axis of [-4 4 1] (FFT image in Fig. 4C). The angle between the two facets was 30°, which matched well with the theoretical values of 27.7°. The typical plane distances of 2.66, 2.53, and 1.50 Å could be

assigned to the *d*-value of (130), (021), and (151) planes of goethite at a zone axis of [3 -1 2] (FFT image in Fig. 4C). As carbonate concentration increased to 286 mM, the phase compositions were similar, i.e., both hematite and goethite were observed. The fringe spacings of 2.51, 1.61, and 1.59 corresponded to the *d*-value of (110), $(01\bar{8})$, and $(\bar{1}0\bar{8})$ reflection planes of hematite at a zone axis of [-8 8 1] (FFT image in Fig. 4G). The plane distances of 2.65, 2.53, and 1.51 Å were consistent with the *d*-value of (130), (021), and (151) reflection planes of goethite at a zone axis of [3 -1 2] (FFT images in Fig. 4G).

Freshly prepared ferrihydrite was highly aggregated with nanoscale particles (< 10 nm), reflecting its short-range-ordered nature (Figs. 4A and 4B). Carbonate modified the morphology of both hematite and goethite under alkaline condition. In the control system, hematite and goethite displayed regular rhombic (with a length of 50-70 nm and a width of 40-60 nm) and rod-like shapes (with a length of 200-250 nm), respectively (Fig. 4C). These observations are similar with the findings of Das et al. and Wang et al.[33, 35] However, under low and medium carbonate concentration (11.42 and 80 mM), hematite formed ellipsoidal crystals and goethite formed needle-like particles (Figs. 4D and 4E). Under high carbonate concentration (180 and 286 mM), hematite was honeycomb-shape and goethite was rugby-like (Figs. 4F and 4G). It is clear that the presence of carbonate did not change the size of products remarkably, but roughened the morphology of hematite and goethite. The morphological results as well as the mineral compositions of the resulting products revealed by TEM analysis are consistent with the XRD and XAS results.

3.2. Carbonate complexation during ferrihydrite transformation

Carbon exhibits strong absorption bands in the region between 1200 and 1600 cm^{-1} in FTIR analysis (Fig. 5). The weak peak centered ca. 1384 cm^{-1} of fresh prepared ferrihydrite was the typical peak of NO_3^- from reagent $Fe(NO_3)_3 \cdot 9H_2O$ (Figs. 5c, 5e, and 5g).[29] Due to the carbon adsorption (e.g., carbonate and/or atmospheric CO_2), the regions between 1200 and 1600 cm^{-1} in FTIR spectra of fresh ferrihydrite as a function of carbonate concentration split into two peaks, corresponding to the asymmetric (asym) and symmetric (sym) stretching region (Figs. 5a, 5c, 5e, and 5g). Fig. 5a was taken as an example to analyze surface carbonate complex types based on the calculated vibrational frequencies reported by Bargar et al. and Hausner et al.[36, 37] The peaks fell into four frequencies at ca. 1515 cm^{-1}, 1470 cm^{-1}, 1366 cm^{-1}, and 1318 cm^{-1}. The vibrational frequencies at 1515/1318 cm^{-1} ($\triangle \nu \approx 200$ cm^{-1}) corresponded to the asym/sym stretching region of bidentate binuclear inner-sphere complex.[36, 37] The vibrational frequencies at 1470/1366 cm^{-1} ($\triangle \nu \approx 100$ cm^{-1}) assigned to that of outer-sphere complex.[36, 37] Hausner et al. experimentally proved the outer-sphere carbonate surface species could form on ferrihydrite from atmospheric CO_2 when ferrihydrite (prepared under CO_2/carbonate free conditions) was exposed to ambient moisture for ~5 min.[37] It is possible that some of outer-sphere carbonate surface complexes in our sample were contributed from the atmospheric CO_2. However, only weak signals of inner-sphere carbonate complexes were detected regardless of carbonate concentration for aged ferrihydrite (Figs. 5b, 5d, 5f, and 5h), indicating that outer-sphere carbonate species from atmospheric CO_2 could be ignored. These results suggested exogenous carbonate formed both bidentate binuclear inner-sphere and outer-sphere

complexes on fresh ferrihydrite at 0d. But no obvious increase in the signal of carbonate complexes was observed with the increasing carbonate concentration, revealing that the adsorption of carbonate on ferrihydrite surface has reached equilibrium at 11.42-286 mM of carbonate. For four aged ferrihydrite (Figs. 5b, 5d, 5f, and 5h), only weak signals of inner-sphere carbonate complexes were detected, probably due to the ligand exchange by terminal hydroxyls on iron octahedrons and/or the desorption by hydroxyl ions in alkaline media, which are discussed in Section 3.3.

3.3. Mechanisms of carbonate effects on the ferrihydrite transformation in alkaline media

The LCF analysis of EXAFS spectra revealed that nitrate did not influence the transformation of ferrihydrite (Figs. S7-S9 and Table S1). In the presence of nitrate within 0.32-268 mM, ferrihydrite completely transformed to 89-91% of goethite and 9-11% of hematite within 10d, which were almost identical with the control system (Fig. S7 and Table S1). This reveals that, on the mineral surface, the effects of minor residual nitrate on the transformation process could be neglected. Therefore, it is clear that in alkaline media carbonate inhibited the ferrihydrite transformation slightly and suppressed the goethite formation, but enhanced the hematite formation regardless of its concentration. Specifically, low carbonate addition (11.42 mM) promoted the hematite generation and inhibited the goethite generation markedly. Whereas at carbonate concentration beyond 11.42 mM, the enhancement impact on hematite and inhibitory effect on goethite were retarded.

It is widely accepted that ferrihydrite transforms to goethite via dissolution and

recrystallization, and to hematite via dehydration and internal atomic rearrangement (Fig. 6A).[13, 14, 38] In the control system, goethite (90%) was the primary transformation product. This is because alkaline condition favored ferrihydrite dissolution from monovalent Fe(III) ions ($Fe(OH)_4^-$).[13] Carbonate inhibited the ferrihydrite transformations slightly, as the transformation efficiency of ferrihydrite decreased from 100% to 79-86% as carbonate concentration increased from 0 to 286 mM. This was different from the previous studies conducted at near-neutral pH under the same other conditions (i.e., reactant concentration and temperature), which observed the enhanced transformation of ferrihydrite by carbonate.[34, 39] The rate of ferrihydrite transformation in the absence of coexisting substances increases with increasing pH and temperature.[13-15, 33] Investigations using other oxyanions (i.e., phosphate, silicate, and arsenic) with much lower content (e.g., P/Fe = 0.075, Si/Fe = 0.025, As/Fe = 0.050) suggested that such oxyanions could inhibit or prevent directly the ferrihydrite transformation at alkaline pH 10-12 under 50-80 °C (higher than 40 °C in current study).[2, 28, 40] However, in this study, in the presence of carbonate with C/Fe = 0.114 - 2.860 at pH 10, 40 °C, transformation efficiency of ferrihydrite achieved the range of 79-86%. The different results obtained in this study were because although alkaline condition favored the dissolution of pure ferrihydrite from $Fe(OH)_4^-$ and accelerated the transformation of ferrihydrite to goethite linearly, the coexisting carbonate inhibited the goethite formation but enhanced the hematite formation with different extent (Figs. 1 and 2).

Interestingly, carbonate concentration of 11.42 mM is vital for the contents of transformation products. Specifically, carbonate promoted the hematite formation from 10%

to 59% but inhibited the goethite formation from 90% to 21%. Based on FTIR analysis, carbonate formed both bidentate binuclear inner-sphere and outer-sphere complexes at 0d on ferrihydrite. The inner-sphere carbonate ligands could hinder the ferrihydrite dissolution and thus inhibit the goethite nucleation (Fig. 6B), which was similar with the inhibition effect on the goethite formation induced by other inner-sphere ligands like phosphate, silicate, and arsenic.[2, 40, 41] The hematite formation involves an internal dehydration/rearrangement process within iron octahedrons in ferrihydrite.[13, 14, 38] A terminal hydroxyl ligand of an iron octahedron is displaced with a terminal hydroxyl ligand of another iron octahedron to form a linkage between two iron octahedrons and water molecule (Eq. (3)).

$$\equiv Fe - OH + \equiv Fe - OH \rightarrow \equiv Fe - O - Fe\equiv + H_2O \quad (3)$$

Where ≡ is the rest of an iron octahedron structure. It occurs regardless of the charge of FeO_6 reactants since this is a Fe-O bond breaking reaction. At alkaline pH, carbonate forms deprotonated species on ferrihydrite surface.[36] The shared charge (the valence of the central atom divided by the number of bonded O atoms) of a hydroxyl ion is 1/1= +1 (Fig. S10).[42] Carbonate has a shared charge of 4/3 = 1.33 (Fig. S10). The smaller the shared charge, the greater the effective negative charge residing on each O atom.[42] Therefore, it forms a stronger metal-oxyanion ionic bond on mineral surface.[42] In a carbonate ion and a hydroxyl ion, the effective negative charge residing on an O atom is -0.67 and -1, respectively (Fig. S10). The Fe-O of hydroxyl is stronger than that of carbonate. Therefore, adsorbed bidentate binuclear

inner-sphere carbonate complex can be easily replaced with two terminal hydroxyl ligands, resulting in an enhanced rearrangement reaction and hematite formation (Eq. (4), Fig. 6B).

$$\equiv Fe_2O_2CO + 2(\equiv Fe - OH) \rightarrow 2(\equiv Fe - O - Fe\equiv) + 2H^+ + CO_3^{2-} \quad (4)$$

However, at carbonate concentration > 11.42 mM, the inhibitory effect on goethite and the enhancement effect on hematite were retarded (Fig. 6C). On the one hand, adsorption equilibrium of carbonate on ferrihydrite surface at 0d (FTIR results) probably inhibited the terminal ligand exchange between adsorbed carbonate and terminal hydroxyls on iron octahedrons, resulting in the slow increase in hematite formation at 80-286 mM of carbonate. On the other hand, during the ferrihydrite transformation, most of carbonate were replaced by terminal hydroxyl ligands on iron octahedrons (Eq. (4)) and/or desorbed by hydroxyl ions in alkaline mineral suspensions (Eq. (5), FITR results).[42, 43] The replacement and desorption of carbonate also resulted in the weak effect on goethite and hematite formation.

$$\equiv Fe_2O_2CO + 2OH^- \rightarrow 2(\equiv Fe - OH) + CO_3^{2-} \quad (5)$$

Under alkaline condition, carbonate modified the morphology of hematite and goethite from typical rhombic and rod-like to less regular morphology with rough surfaces (Fig. 4). This is inconsistent with the previous studies that found carbonate promoted the formation of crystalline rhombic hematite at near-neutral pH.[34, 39] In mineral suspensions at alkaline pH,

inner-sphere adsorption of carbonate, replacement by terminal hydroxyl ligands, and/or desorption by hydroxyl ions occurred simultaneously and rapidly on the reactive sites of ferrihydrite and transformation products. This may alter the transformation of ferrihydrite through oriented attachments and the crystal face growth of goethite and hematite, and thus roughen the morphologies of products.[41, 44, 45]

4. Conclusions

In a broad context, in alkaline media like arid and semiarid soils, radioactive waste disposal systems, mine tailings, and metallurgical operations, ferrihydrite easily forms and plays a significant role in the sequestration of nutrients and hazardous elements such as phosphorus, actinides, and heavy metals due to its high surface area. However, ferrihydrite is metastable solid and readily transforms into crystalline phases, which lowers the surface area of reactive absorbent.[33, 39] Different from the strong inhibitory effect on the ferrihydrite transformation induced by phosphate, silicate, and arsenic in alkaline media,[2, 28, 40] this study clearly showed that carbonate slowed down the ferrihydrite transformation slightly and suppressed the goethite formation, however, promoted the hematite formation regardless of its concentration. During the ferrihydrite transformation, hazardous elements (e.g., As) could be incorporated into the structure of hematite.[3, 4, 18] By promoting the hematite formation, the presence of carbonate may potentially provide a pathway through which hazardous elements can be retained as ferrihydrite transforms. This study not only fills the knowledge gap of how increasing carbonate changes iron (oxyhydr)oxide transformation in natural and engineered alkaline settings, but also provides the implications for the immobilization and release of

contaminants.

Author contributions

Ying Li: Conceptualization, Data curation, Formal analysis, Funding acquisition, Investigation, Methodology, Project administration, Resources, Software, Validation, Writing - original draft, and Writing - review & editing. Chaoqun Zhang: Formal analysis, Investigation, and Methodology. Meijun Yang: Formal analysis, Investigation, and Methodology. Jing Liu: Formal analysis and Methodology. Hongping He: Conceptualization. Yibing Ma: Conceptualization. Yuji Arai: Conceptualization, Data curation, Funding acquisition, Methodology, Project administration, Resources, Supervision, Writing - original draft, and Writing - review & editing.

Conflicts of interest

There are no conflicts to declare.

Acknowledgements

This work was supported by the Science and Technology Development Fund, Macau SAR (0037/2023/RIA1 and 001/2022/NIF), the United States Department of Agriculture (# ILLU-875-971), and the Macau University of Science and Technology Faculty Research Grants (FRG-23-035-FIE). Use of the Advanced Photon Source was supported by the U. S. Department of Energy, Office of Science, Office of Basic Energy Sciences, under Contract No. DE-AC02-06CH11357.

References

1 J. López-Bucio, A. Guevara-García, V. Ramírez-Rodríguez, M. Nieto and L. Herrera-Estrella In Agriculture for marginal lands: transgenic plants towards the third millennium, Plant genetic engineering: towards the third millennium: Proceedings of the International Symposium on Plant Genetic Engineering, Havana, Cuba, 6-10 December, 1999, *Elsevier Science Publishers*, 2000, 159-165.

2 P. C. M. Francisco, T. Sato, T. Otake and T. Kasama, Kinetics of Fe^{3+} mineral crystallization from ferrihydrite in the presence of Si at alkaline conditions and implications for nuclear waste disposal, *Am. Mineral.*, 2016, **101**, 2057-2069.

3 S. Das, J. Essilfie-Dughan and M. J. Hendry, Fate of adsorbed arsenate during phase transformation of ferrihydrite in the presence of gypsum and alkaline conditions, *Chem. Geol.*, 2015, **411**, 69-80.

4 T. A. Marshall, K. Morris, G. T. W. Law, F. R. Livens, J. F. W. Mosselmans, P. Bots and S. Shaw, Incorporation of uranium into hematite during crystallization from ferrihydrite, *Environ. Sci. Technol.*, 2014, **48**, 3724-3731.

5 J. Robertson, M. J. Hendry, J. Essilfie-Dughan and J. Chen, Precipitation of aluminum and magnesium secondary minerals from uranium mill raffinate (pH 1.0–10.5) and their controls on aqueous contaminants, *Appl. Geochem.*, 2016, **64**, 30-42.

6 M. Shi, X. Min, Y. Ke, Z. Lin, Z. Yang, S. Wang, N. Peng, X. Yan, S. Luo and J. Wu, Recent progress in understanding the mechanism of heavy metals retention by iron (oxyhydr)oxides, *Sci. Total Environ.*, 2021, **752**, 141930.

7 G. Chen, A. Thompson and C. A. Gorski, Disentangling the size-dependent redox reactivity of iron oxides using thermodynamic relationships, *PNAS*, 2022, **119**, 2204673119.

8 F. M. Michel, L. Ehm, S. M. Antao, P. L. Lee, P. J. Chupas, G. Liu, D. R. Strongin, M. A. A. Schoonen, B. L. Phillips and J. B. Parise, The structure of ferrihydrite, a nanocrystalline material, *Science*, 2007, **316**, 1726-1729.

9 J. L. Jambor and J. E. Dutrizac, Occurrence and constitution of natural and synthetic ferrihydrite, a widespread iron oxyhydroxide, *Chem. Rev.*, 1998, **98**, 2549-2586.

10 N. Y. Dzade and N. H. De Leeuw, Density functional theory characterization of the structures of H_3AsO_3 and H_3AsO_4 adsorption complexes on ferrihydrite, *Environ. Sci.: Proc. Imp.*, 2018, **20**, 977-987.

11 L. Tian, Z. Shi, Y. Lu, A. C. Dohnalkova, Z. Lin and Z. Dang, Kinetics of cation and oxyanion adsorption and desorption on ferrihydrite: Roles of ferrihydrite binding sites and a unified model, *Environ. Sci. Technol.*, 2017, **51**, 10605-10614.

12 Y. Liang, L. Tian, Y. Lu, L. Peng, P. Wang, J. Lin, T. Cheng, Z. Dang and Z. Shi, Kinetics of Cd(II) adsorption and desorption on ferrihydrite: experiments and modeling, *Environ. Sci.: Proc. Imp.*, 2018, **20**, 934-942.

13 U. Schwertmann and E. Murad, Effect of pH on the formation of goethite and hematite from ferrihydrite, *Clays Clay Miner.*, 1983, **31**, 277-284.

14 U. Schwertmann, H. Stanjek and H. H. Becher, Long-term in vitro transformation of 2-line ferrihydrite to goethite/hematite at 4, 10, 15 and 25°C, *Clay Miner.*, 2004, **39**, 433-438.

15 F. E. Furcas, B. Lothenbach, S. Mundra, C. N. Borca, C. C. Albert, O. B. Isgor, T. Huthwelker and U. M. Angst, Transformation of 2-line ferrihydrite to goethite at alkaline pH, *Environ. Sci. Technol.*, 2023, **57**, 16097-16108.

16 J. Liu, R. Zhu, L. Ma, H. Fu, X. Lin, S. C. Parker and M. Molinari, Adsorption of phosphate and cadmium on iron (oxyhydr)oxides: A comparative study on ferrihydrite, goethite, and hematite, *Geoderma*, 2021, **383**, 114799.

17 J. Liu, J. Cao, W. Yuan, Q. Zhong, X. Xiong, Q. E. Ouyang, X. Wei, Y. Liu, J. Wang and X. Li, Thallium adsorption on three iron (hydr)oxides and Tl isotopic fractionation induced by adsorption on ferrihydrite, *Sci. Total Environ.*, 2023, **871**, 161863.

18 Y. Lu, S. Hu, Z. Liang, M. Zhu, Z. Wang, X. Wang, Y. Liang, Z. Dang and Z. Shi, Incorporation of Pb(II) into hematite during ferrihydrite transformation, *Environ. Sci.: Nano*, 2020, **7**, 829-841.

19 IPCC, Climate Change 2013 - The Physical Science Basis: Summary for Policymakers. Intergovernmental Panel on Climate Change: 2013.

20 J. Xie, Y. Li, C. Zhai, C. Li and Z. Lan, CO_2 absorption by alkaline soils and its implication to the global carbon cycle, *Environ. Geol.*, 2008, **56**, 953-961.

21 E. Maryol and C. Lin, Evaluation of atmospheric CO_2 sequestration by alkaline soils through simultaneous enhanced carbonation and biomass production, *Geoderma*, 2015, **241-242**, 24-31.

22 X. Zhao, C. Zhao, J. Wang, K. Stahr and Y. Kuzyakov, $CaCO_3$ recrystallization in saline and alkaline soils, *Geoderma*, 2016, **282**, 1-8.

23 J. P. Gustafsson, Visual MINTEQ 3.1 [online] http://www.vminteq.lwr.kth.se/visual-minteq-ver-3-1/, Department of Land and Water Recources, KTH Royal Institute of Technology, Stockholm, Sweden, 2013.

24 M. Villalobos, M. A. Trotz and J. O. Leckie, Surface complexation modeling of carbonate effects on the adsorption of Cr(VI), Pb(II), and U(VI) on goethite, *Environ. Sci. Technol.*, 2001, **35**, 3849-3856.

25 S. Namgung, B. Guo, K. Sasaki, S. S. Lee and G. Lee, Macroscopic and microscopic behaviors of Mn(II) (ad)sorption to goethite with the effects of dissolved carbonates under anoxic conditions, *Geochim. Cosmochim. Acta*, 2020, **277**, 300-319.

26 Y. Arai, D. L. Sparks and J. A. Davis, Effects of dissolved carbonate on arsenate adsorption and surface speciation at the hematite-water interface, *Environ. Sci. Technol.*, 2004, **38**, 817-824.

27 H. Wijnja and C. P. Schulthess, Effect of carbonate on the adsorption of selenate and sulfate on goethite, *Soil Sci. Soc. Am. J.*, 2002, **66**, 1190-1197.

28 S. Das, M. J. Hendry and J. Essilfie-Dughan, Effects of adsorbed arsenate on the rate of transformation of 2-line ferrihydrite at pH 10, *Environ. Sci. Technol.*, 2011, **45**, 5557-5563.

29 U. Schwertmann and R. M. Cornell, Iron oxides in the laboratory: Preparation and characterization, 2000.

30 J. Murillo-Gelvez, D. M. Di Toro, H. E. Allen, R. F. Carbonaro and P. C. Chiu, Reductive transformation of 3-nitro-1,2,4-triazol-5-one (NTO) by leonardite humic acid and anthraquinone-2,6-disulfonate (AQDS), *Environ. Sci. Technol.*, 2021, **55**, 12973-12983.

31 S.-Y. Oh, P. C. Chiu, B. J. Kim and D. K. Cha, Zero-valent iron pretreatment for enhancing the biodegradability of RDX, *Water Res.*, 2005, **39**, 5027-5032.

32 B. Ravel and M. Newville, ATHENA, ARTEMIS, HEPHAESTUS: Data analysis for X-ray absorption spectroscopy using IFEFFIT, *J. Synchrotron Radiat.*, 2005, **12**, 537-541.

33 S. Das, M. J. Hendry and J. Essilfie-Dughan, Transformation of two-line ferrihydrite to goethite and hematite as a function of pH and temperature, *Environ. Sci. Technol.*, 2011, **45**, 268-275.

34 Y. Li, C. Zhang, M. Yang, H. He and Y. Arai, Carbonate accelerated transformation of ferrihydrite in the presence of phosphate, *Geoderma*, 2022, **417**, 115811.

35 X. Wang, M. Zhu, S. Lan, M. Ginder-Vogel, F. Liu and X. Feng, Formation and secondary mineralization of ferrihydrite in the presence of silicate and Mn(II), *Chem. Geol.*, 2015, **415**, 37-46.

36 J. R. Bargar, J. D. Kubicki, R. Reitmeyer and J. A. Davis, ATR-FTIR spectroscopic characterization of coexisting carbonate surface complexes on hematite, *Geochim. Cosmochim. Acta*, 2005, **69**, 1527-1542.

37 D. B. Hausner, N. Bhandari, A.-M. Pierre-Louis, J. D. Kubicki and D. R. Strongin, Ferrihydrite reactivity toward carbon dioxide, *J. Colloid Interface Sci.*, 2009, **337**, 492-500.

38 Y. Cudennec and A. Lecerf, The transformation of ferrihydrite into goethite or hematite, revisited, *J. Solid State Chem.*, 2006, **179**, 716-722.

39 Y. Li, M. Yang, M. Pentrak, H. He and Y. Arai, Carbonate-enhanced transformation of ferrihydrite to hematite, *Environ. Sci. Technol.*, 2020, **54**, 13701-13708.

40 C. R. Paige, W. J. Snodgrass, R. V. Nicholson, J. M. Scharer and Q. H. He, The effect of phosphate on the transformation of ferrihydrite into crystalline products in alkaline media, *Water Air Soil Pollut.*, 1997, **97**, 397-412.

41 A. Namayandeh, O. J. Borkiewicz, N. M. Bompoti, M. Chrysochoou and F. M. Michel, Oxyanion surface complexes control the kinetics and pathway of ferrihydrite transformation to goethite and hematite, *Environ. Sci. Technol.*, 2022, **56**, 15672-15684.

42 M. B. McBride, Environmental Chemistry of Soils, 1994.

43 M. Villalobos and J. O. Leckie, Carbonate adsorption on goethite under closed and open CO_2 conditions, *Geochim. Cosmochim. Acta*, 2000, **64**, 3787-3802.

44 D. G. Lewis and U. Schwertmann, The effect of [OH] on the goethite produced from ferrihydrite under alkaline conditions, *J. Colloid Interface Sci.*, 1980, **78**, 543-553.

45 J. A. Soltis, J. M. Feinberg, B. Gilbert and R. L. Penn, Phase transformation and particle-mediated growth in the formation of hematite from 2-line ferrihydrite, *Cryst. Growth Des.*, 2016, **16**, 922-932.

Figures

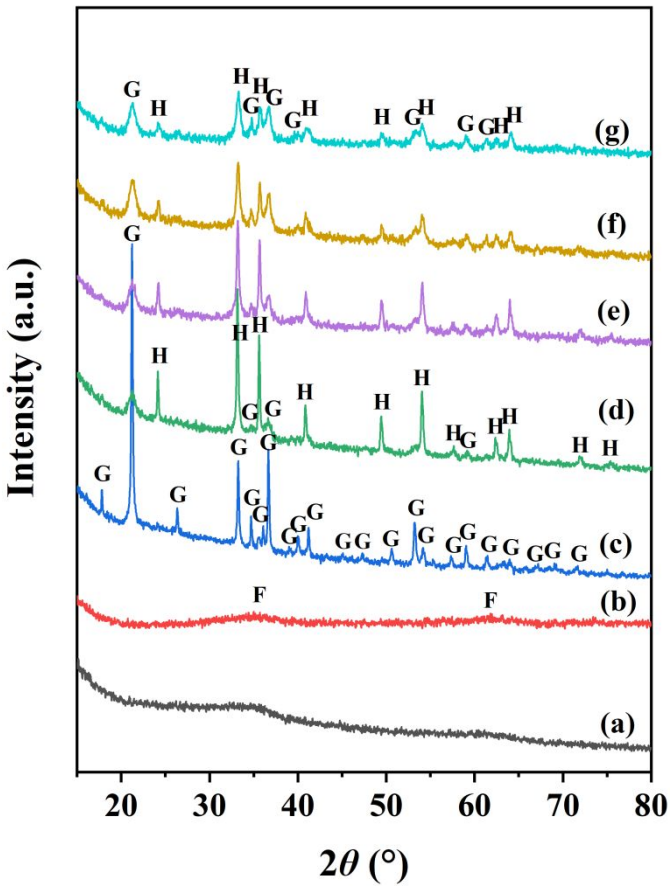

Fig. 1. XRD patterns of ferrihydrite as a function of carbonate concentration of (a) 0 mM (control) at 0d, (b) 286 mM at 0d, (c) 0 mM at 21d, (d) 11.42 mM at 21d, (e) 80 mM at 21d, (f) 180 mM at 21d, (g) 286 mM at 21d. Ferrihydrite, goethite, and hematite are abbreviated as F, G, and H, respectively.

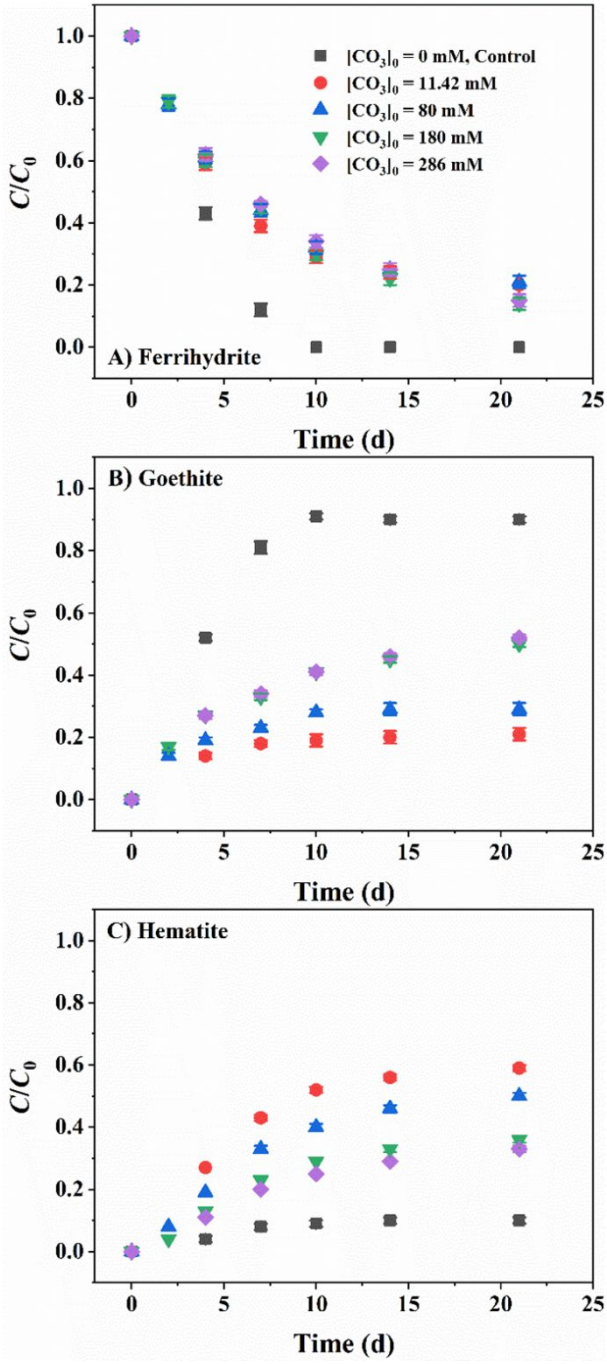

Fig. 2. Effects of carbonate concentration on A) ferrihydrite transformation, B) goethite formation, and C) hematite formation at pH 10. C_0 is the percent ferrihydrite before phase transformation (100%), and C is the relative amount of iron (oxyhydr)oxides remaining or generating at aging time t (d) calculated using the LCF of Fe K-edge EXAFS spectra. Carbonate is abbreviated as CO_3. Meaning of symbols in panels B) and C) are the same with panel A).

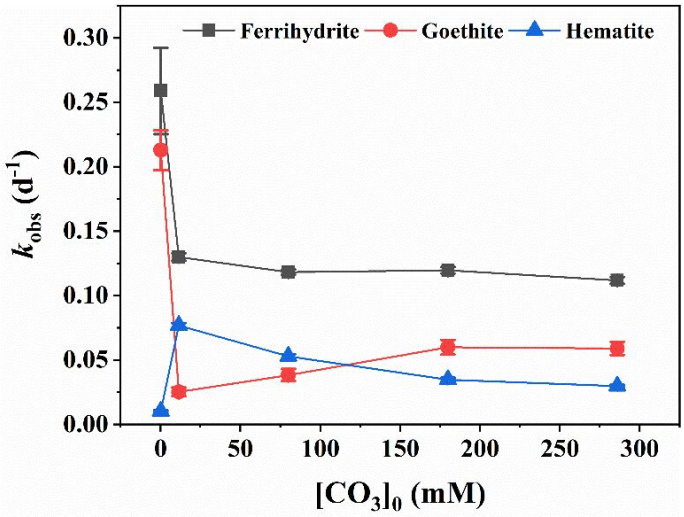

Fig. 3. Effects of carbonate concentration on the first-order reaction rate constant (k_{obs}) of ferrihydrite transformation and products formation within 10d. Carbonate is abbreviated as CO_3.

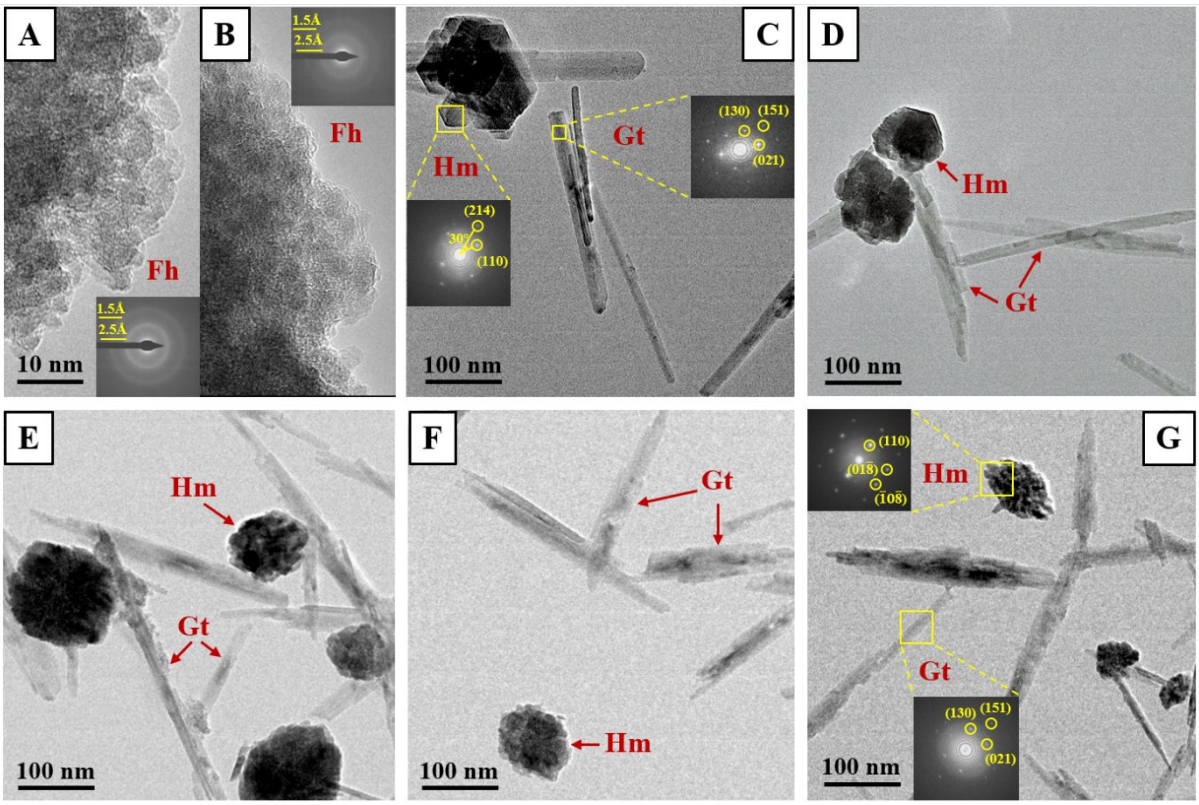

Fig. 4. TEM images of ferrihydrite as a function of carbonate concentration of A) 0 mM (control) at 0d, B) 286 mM at 0d, C) 0 mM at 21d, D) 11.42 mM at 21d, E) 80 mM at 21d, F) 180 mM at 21d, and G) 286 mM at 21d. Insets in panels A) and B) are SAED images. Insets in panels C) and G) are FFT images. Ferrihydrite, goethite, and hematite are abbreviated as Fh, Gt, and Hm, respectively.

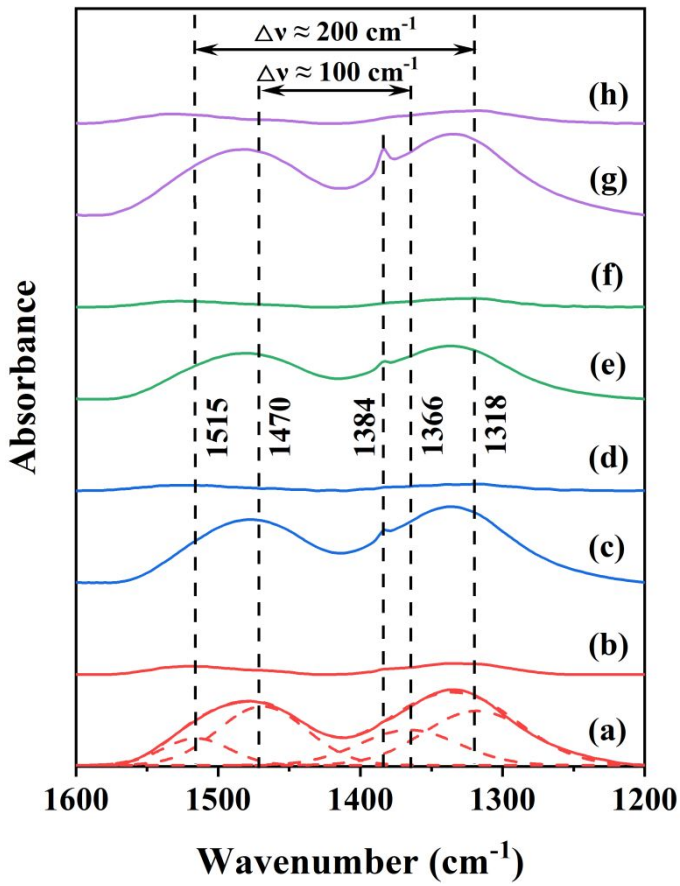

Fig. 5. FTIR spectra of ferrihydrite as a function of carbonate concentration of (a) 11.42 mM at 0d, (b) 11.42 mM at 21d, (c) 80 mM at 0d, (d) 80 mM at 21d, (e) 180 mM at 0d, (f) 180 mM at 21d, (g) 286 mM at 0d, and (h) 286 mM at 21d.

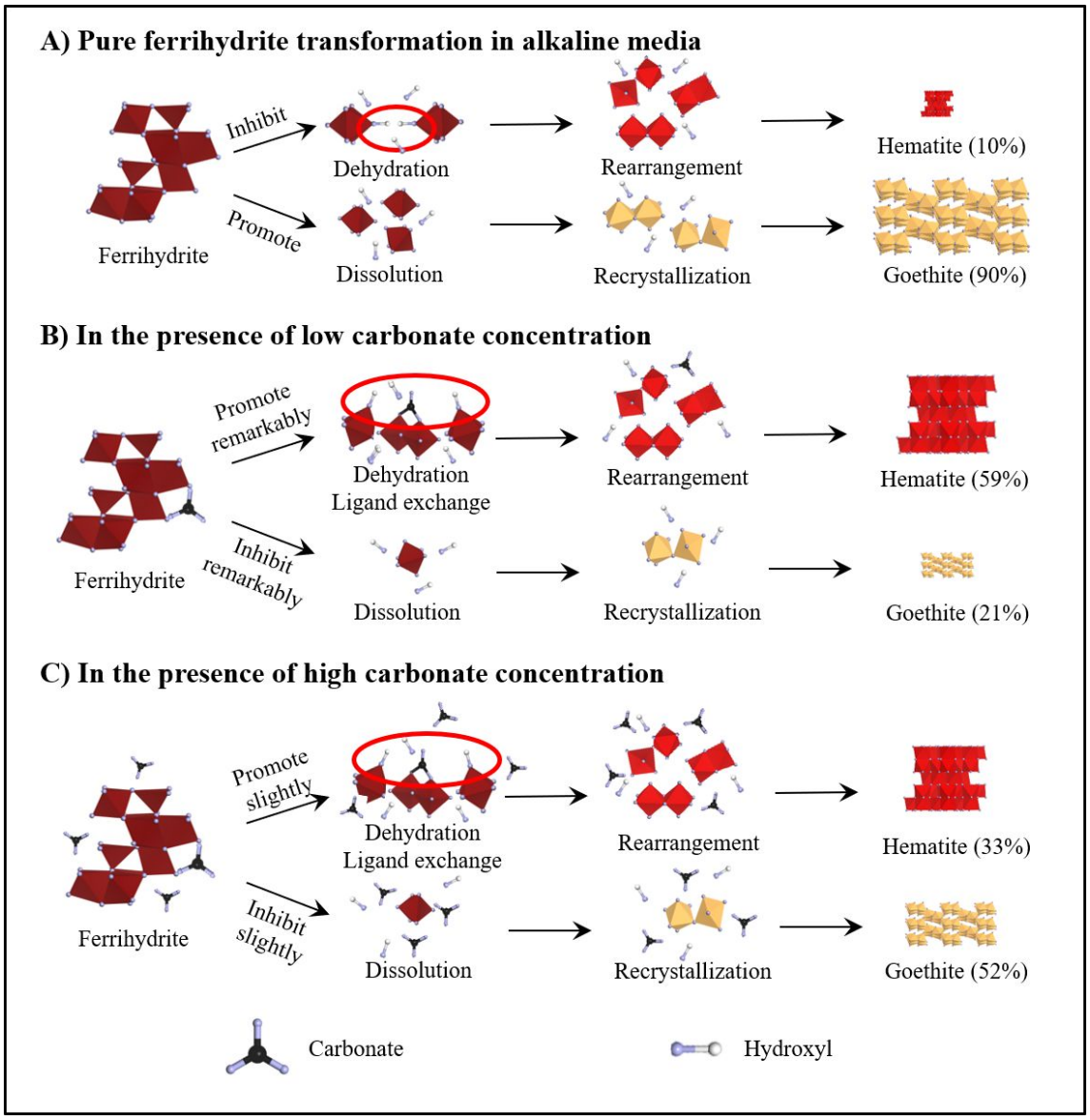

Fig. 6. Schematic figures for A) ferrihydrite transformation in the absence of carbonate, B) ferrihydrite transformation in the presence of low carbonate concentration (11.42 mM), and C) ferrihydrite transformation in the presence of high carbonate concentration (286 mM) in alkaline media.